Strain Energy Band Engineering in AlGaInN/GaN Heterostructure Field Effect Transistors

M. Asif Khan, [a] M. S. Shur, [b] and R. Gaska [b]

[a] Department of ECE, University of South Carolina, Columbia, South Carolina 29208, USA
[b] Department of ECSE, Rensselaer Polytechnic Institute, Troy, New York 12180, USA

Abstract.

We report on $Al_xIn_yGa_{1-x-y}N$-GaN heterojunctions grown on sapphire and 6H/4H SiC substrates using a low pressure MOCVD. Based on a linear extrapolation of lattice constants as functions of molar fractions, we estimate that quaternary $Al_xIn_yGa_{1-x-y}N$ layers with Al/In mole fraction ratio of 5 should be nearly lattice-matched to GaN. The independent control of strain and of the band offset has been confirmed by X-ray and photoluminescence data. For $Al_xIn_yGa_{1-x-y}N$-GaN junctions with barrier thickness less than 50 nm and varying alloy compositions (x from 0.1 to 0.2 and y from 0.00 to 0.02), room temperature sheet-carrier density and mobility values ranging from 0.5-1.5 x 10^{13} cm $^{-2}$ and 1000-1500 $cm^2V^{-1}sec^{-1}$ were measured. The mobility values increase by about a factor of 5 upon cooling to 77 K. This establishes the presence of the two-dimensional electron gas at the $Al_xIn_yGa_{1-x-y}N$-GaN heterojunction interface and confirms a high quality of heterointerfaces. We also fabricated $Al_xIn_yGa_{1-x-y}N$-GaN HFETs with the state-of-the art performance. The fabrication technology for these devices is substantially different from that for conventional AlGaN/GaN HEMTs. We will report on DC and microwave characteristics of these devices and compare these characteristics with those for conventional GaN-based HFETs.

Introduction.

The large lattice mismatch between GaN, AlN and InN and the strong piezoelectric effects in these materials significantly impact the electrical properties of III-N Heterostructure Field Effect Transistors. In GaN/AlGaN heterostructures, strain-induced sheet carrier concentration can exceed $1x10^{13}$ cm^{-2} (see Fig. 1) and the overall sheet carrier density can exceed the values typical for the AlGaAs/GaAs materials system by more than an order of magnitude, see Fig. 2.

The effect, referred to as piezoelectric doping, can be used to enhance the maximum current carrying capabilities. On the other hand, our experimental and theoretical data point out to a gradual strain relaxation when the critical thickness for the development of the misfit dislocation is approached. This might affect the device performance, stability, and reliability, and cause the long-term instabilities that several groups observed in their AlGaN/GaN HFETs. Therefore, nearly all the reported HEMT devices to date use strained GaN-AlGaN junctions with alloy compositions below 35 % and 15-20 nm thick barriers to avoid exceeding or even approaching too closely the critical thickness. Our group has developed a technique that should allow us to independently control strain and lattice mismatch in GaN-based HFETs. To this end, we used $Al_xIn_yGa_{1-x-y}N$-GaN heterojunctions grown on sapphire and 6H/4H SiC substrates using a low pressure MOCVD. Based on a linear extrapolation of lattice constants as functions of molar fractions, we estimate that quaternary $Al_xIn_yGa_{1-x-y}N$ layers with Al/In mole fraction ratio of 5 should be nearly lattice-matched to GaN.

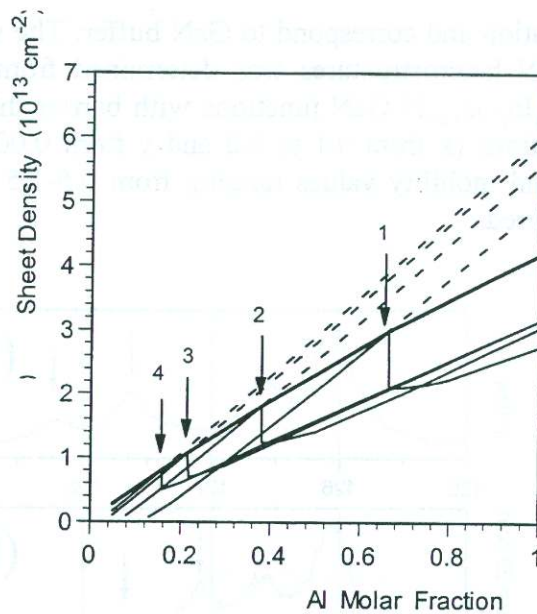

Fig. 1. Electron sheet density, n_s, induced by polarization in $Al_xGa_{1-x}N$-GaN heterostructures with different aluminum molar fractions and various AlGaN barrier layer thicknesses: 1 - 30 nm; 2 - 20 nm; 3 - 10 nm; 4 - 5 nm. Arrows show the onset of the strain relaxation. Thick solid line shows sheet electron density corresponding to critical thickness of AlGaN versus aluminum molar fraction. Dashed lines show n_s for unrelaxed heterostructures. [1]

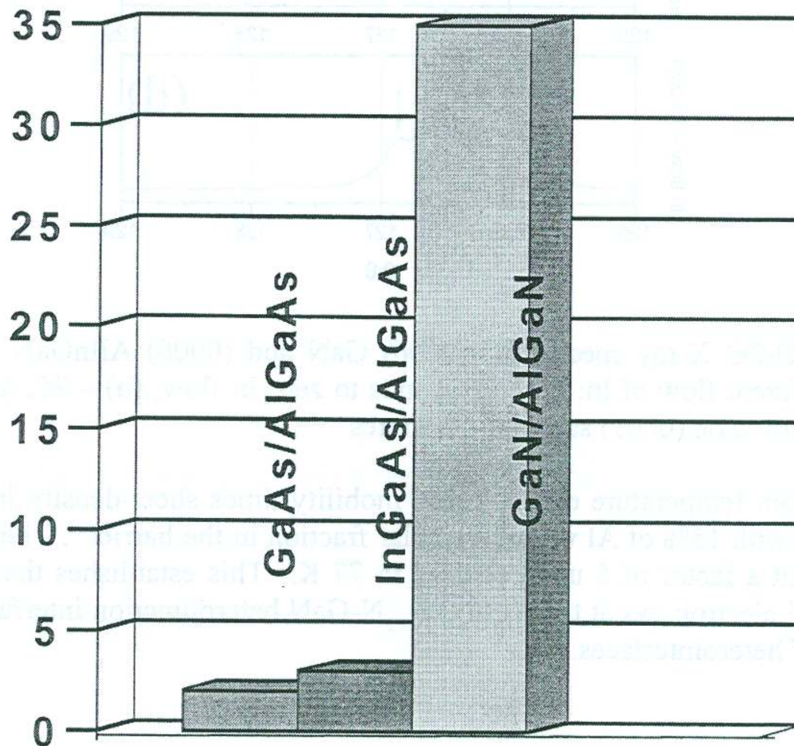

Fig. 2. Maximum value of n_s in different heterostructure systems. [2]

The independent control of strain and of the band offset has been confirmed by X-ray and photoluminescence data. Fig. 3 shows Θ-2Θ X-ray spectra of (0006) GaN and (0006) AlInGaN with 9% of Al, deposited at different flow of In [3]. Arrows mark peaks corresponding to AlInGaN layers with different In content. The other two peaks do not

depend on In incorporation and correspond to GaN buffer. The variation of the energy band-offset in AlInGaN/GaN heterostructures was determined from photoluminescence spectra (see Fig. 4) [3]. For $Al_xIn_yGa_{1-x-y}N$-GaN junctions with barrier thickness less than 50 nm and varying alloy compositions (x from 0.1 to 0.2 and y from 0.00 to 0.02), room temperature sheet-carrier density and mobility values ranging from 0.5-1.5 x 10^{13} cm $^{-2}$ and 1000-1500 $cm^2V^{-1}sec^{-1}$ were measured.

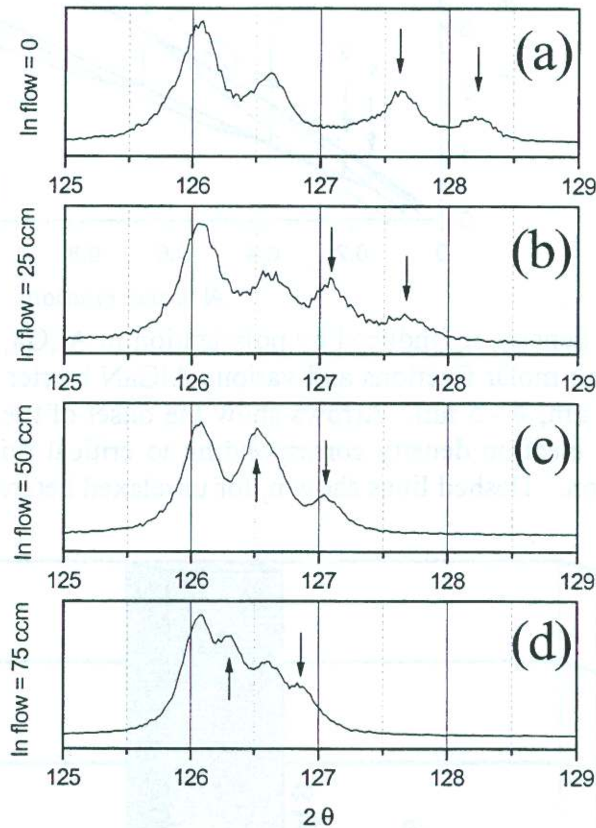

Fig. 3. Fig. 3. Θ-2Θ X-ray spectra of (0006) GaN and (0006) AlInGaN with 9% of Al, deposited at different flow of In: (a) corresponds to zero In flow, (b) – 25; (c) – 50; (d) –75. Samples were grown on (0001) sapphire substrates

Fig. 5 shows room temperature electron Hall mobility times sheet-density in AlInGaN/GaN heterostructures with 15% of Al versus In molar fraction in the barrier [4]. The mobility values increase by about a factor of 5 upon cooling to 77 K. This establishes the presence of the two-dimensional electron gas at the $Al_xIn_yGa_{1-x-y}N$-GaN heterojunction interface and confirms a high quality of heterointerfaces.

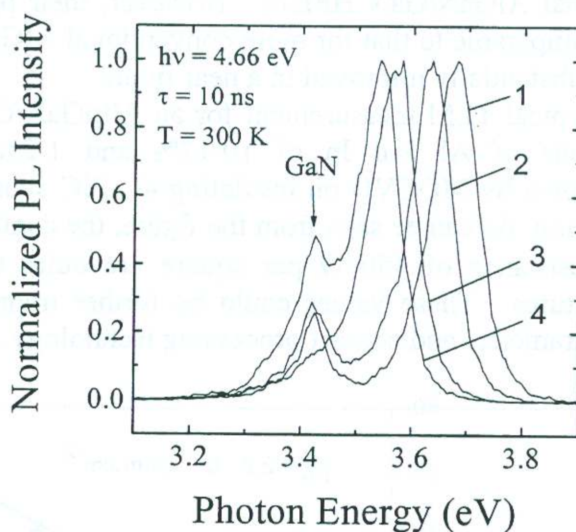

Fig. 4. Normalized room temperature photoluminescence spectra of AlInGaN with 9% of Al on GaN. Curve 1 corresponds to zero In flow, 2 – 25; 3 – 50; 4 –75

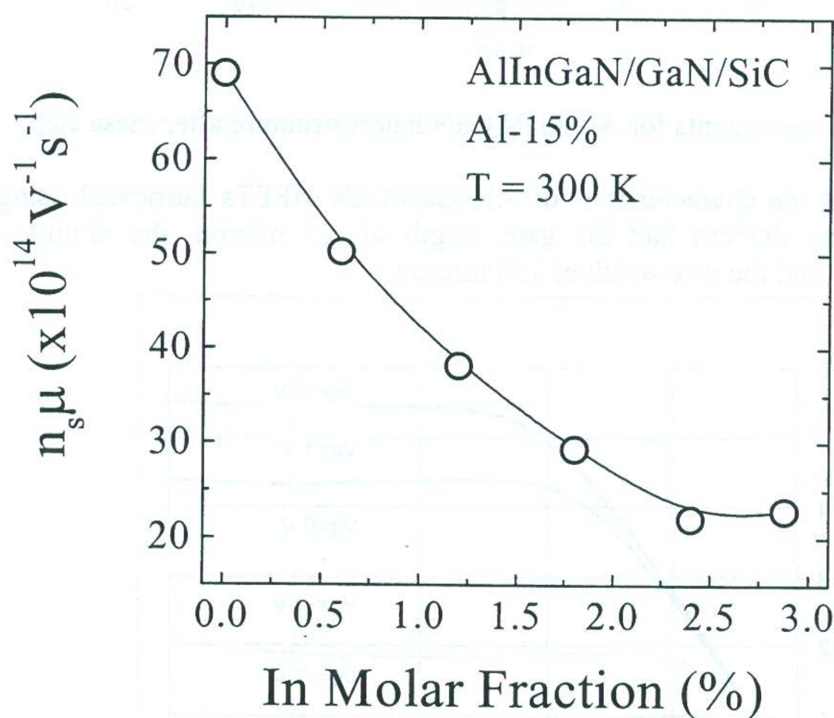

Fig. 5. Room-temperature electron-mobility (Hall) times sheet-density in AlInGaN/GaN heterostructures with 15% of Al versus In molar fraction in the barrier. Samples were grown on 6H-SiC substrates

The growth and fabrication technology for AlInGaN/GaN HFETs are substantially different from that for conventional AlGaN/GaN HFETs. However, their performance achieved on exploratory devices is comparable to that for more conventional AlGaN/GaN HFETs, and we project that it could be substantially improved in a near future.

Fig. 6 shows a typical TLM measurement for an AlInGaN/GaN heterostructure with estimated molar fractions of Al and In of 10-12% and 1-2%, respectively. These heterostructures were grown by MOCVD on insulating 4H-SiC substrates. An approximate barrier thickness was 30 nm. As can be seen from the figure, the contact resistance of $2.2x10^{-5}$ Ωcm^{-2} and the sheet resistance of 450 Ω per square are quite typical for conventional AlGaN/GaN heterostructures. These values could be further improved by optimizing the wide band gap barrier parameters and contact processing technology.

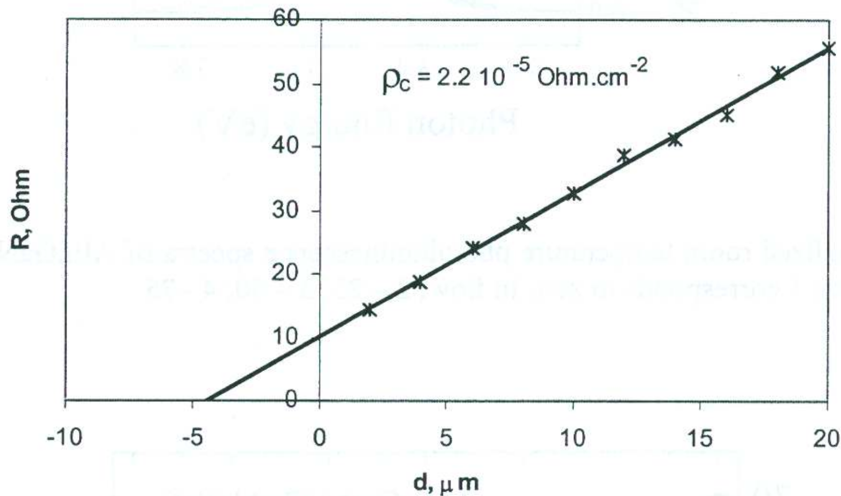

Fig. 6. TLM measurements for AlInGaN/GaN heterostructure after mesa etch.

Figures 7, 8, 9 present the characteristics of AlInGaN/GaN HFETs fabricated using these heterostructures. These devices had the gate length of 1.5 micron, the drain-to-source separation of 3 micron, and the gate width of 150 micron.

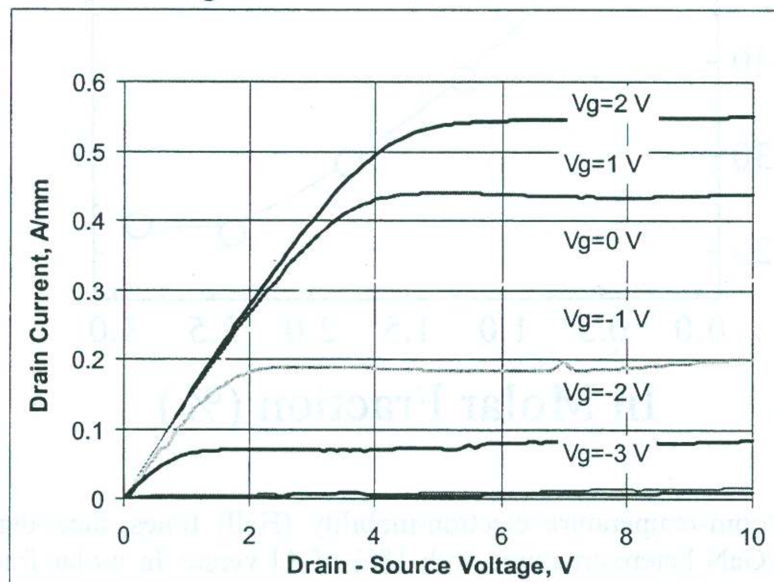

Fig. 7. I-V characteristics of AlInGaN/GaN HFET

The devices have reasonable current values that could be enhanced by increasing the Al molar fraction in order to enhance the piezoelectric doping and the bandgap offset. The use of SiC substrate resulted in a very low self-heating because of superior thermal conductivity of 4H-SiC as evidenced by a very low positive (nearly zero) output conductance. The devices exhibit a very nice pinch-off at approximately – 4 V gate bias. The current modulation in the linear regime and relatively low knee voltages show that the I-V characteristics are determined by the channel resistance. The leakage current is quite low even at the gate bias of 2 V (approximately 2 mA). At – 10 V, the gate leakage was 5 microamps.

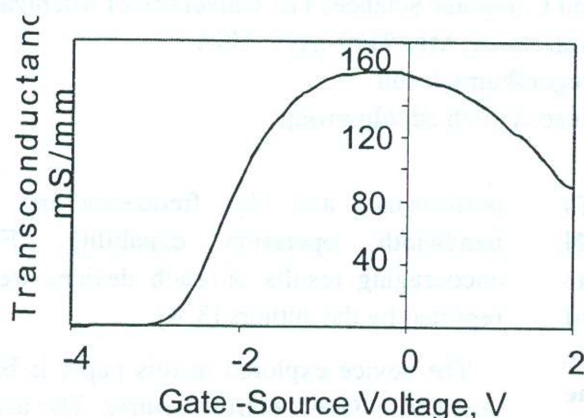

Fig. 8. Transconductance versus gate-to-source voltage. Drain-to-source voltage 5 V

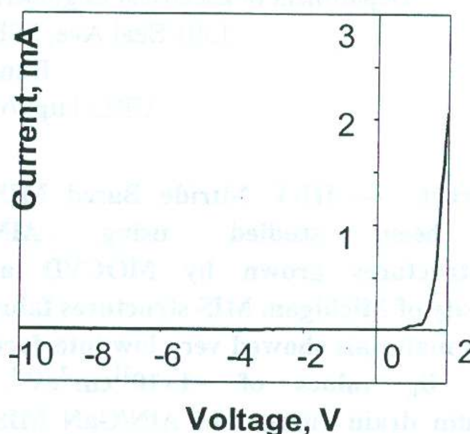

Fig. 9. Gate current-voltage characteristics.

The maximum transconductance is reached at approximately –1.5 V of the gate bias. This shows that it is limited by the maximum sheet charge induced in the channel. Hence, once again, we conclude that the transconductance can be enhanced by increasing Al molar fraction and, possibly, decreasing the thickness of the wide band gap barrier layer, especially for shorter gate devices.

In conclusion, our data clearly demonstrate that state-of-the-art GaN-based HFETs can be fabricated using an AlINGaN wide band gap layer. This allows us to independently control strain and the bandgap offset in these devices and improve their performance.

Acknowledgment. We are grateful to Drs. J. W. Yang, G. Simin and Mr. X. Hu who helped with sample fabrication and characterization. The work at Rensselaer Polytechnic Institute was partially supported by the Office of Naval Research (Project Monitor Dr. Colin Wood)

References.

[1] M. S. Shur, A. D. Bykhovski, R. Gaska, and M. A. Khan, GaN-based Pyroelectronics and Piezoelectronics, in Semiconductor Homo- and Hetero-Device Structures, M. Francombe and C. E. C. Wood, Editors, to be published

[2] M. S. Shur, A. D. Bykhovski, R. Gaska, Piezoelectric Effects in AlGaN/GaN-based Heterostructure Field Effect Transistors, Electrochemical Society Proceedings, Vol. 98-18, pp. 154-168 (1999)

[3] M. Asif Khan, J. W. Yang, G. Simin, Hans zur Loye, R. Bicknell-Tassius, R. Gaska, M. S. Shur, G. Tamulaitis, and A. Zukauskas, "Energy Band/lattice Mismatch Engineering in Quaternary AlInGaN/GaN Heterostructure", ICNS3, Montpellier, France, July 5-9 (1999), to be published in physica status solidi

[4] M. Asif Khan, J. W. Yang, G. Simin, R. Gaska, M. S. Shur, Hans zur Loye, G. Tamulaitis, A. Zukauskas, D. Smith, R. Bicknell-Tassius, "Lattice and Energy Band Engineering in AlInGaN/GaN Heterostructures", submitted for publication